Reexamination of the Electronic Structure of $Bi_2Sr_2CaCu_2O_{8+\delta}$ and $Bi_2Sr_2Cu_1O_{6+\delta}$: Electronlike Portions of the Fermi Surface and Depletion of Spectral Weight near $\bar{M}$

Y.-D. Chuang,[1] A. D. Gromko,[1] D. S. Dessau,[1] Y. Aiura,[2] Y. Yamaguchi,[2] K. Oka,[2] A. J. Arko,[3] J. Joyce,[3] H. Eisaki,[4] S. I. Uchida,[4] K. Nakamura,[5] and Yoichi Ando[5]

[1]*Department of Physics, University of Colorado, Boulder, Colorado 80309-0390*

[2]*Electrotechnical Laboratory (ETL), 1-1-4 Umezono, Tsukuba, Ibaraki 305, Japan*

[3]*Los Alamos National Laboratory, Los Alamos, New Mexico 87545*

[4]*Department of Superconductivity, University of Tokyo, 7-3-1 Hongo, Bunkyo-ku, Tokyo 113, Japan*

[5]*Central Research Institute of Electric Power Industry (CRIEPI), 2-11-1 Iwato-Kita, Komae, Tokyo 201-8511, Japan*

(Received 8 March 1999)

We present a reexamination of the electronic structure and Fermi surface (FS) topology of Bi-Sr-Ca-Cu-O (BSCCO) as obtained from angle-resolved photoemission experiments. By applying a stricter set of FS crossing criteria as well as by varying the incident photon energy outside the usual range, we have found very different behavior from that previously observed. In particular, we have found a FS that is centered around the Γ point and contains electronlike portions, and we observe a depletion of spectral weight around $\bar{M}$. The flat bands observed at other photon energies may indicate the presence of two electronic components in the cuprates.

PACS numbers: 74.25.Jb, 74.72.Hs, 78.70.Dm, 79.60.Bm

Angle-resolved photoemission spectroscopy (ARPES) has emerged as one of the most powerful tools for unearthing the electronic structure and physics of the high temperature superconductors (HTSC) and other correlated electron systems since it allows one to directly probe the $\vec{k}$ space information of the electronic structure [1]. Major discoveries obtained from ARPES experiments on the HTSC's (mostly BSCCO) have included the observation of flat bands (an extended van Hove singularity or vHs) at or very near the Fermi level [2–4], a superconducting gap with d-wave symmetry [5,6], and an anomalous pseudogap above T_c [7–9]. Such advances are all predicated on a thorough knowledge of the normal-state Fermi surface (FS) topology of these superconductors, which has been almost universally accepted to be a holelike pocket centered around the Brillouin zone corners [(π, π) or X, Y points] [3,4,6–12]. In this Letter we present new results on BSCCO that indicate that this most fundamental assumption of the FS topology is either incorrect or at least oversimplified.

The experiments were mostly performed at the Synchrotron Radiation Center (SRC) in Wisconsin with a few backup experiments performed at the Stanford Synchrotron Radiation Laboratory (SSRL) in California [13]. Most of the $Bi_2Sr_2CaCu_2O_{8+\delta}$ (Bi2212) samples for this study came from CRIEPI, with a portion coming from ETL. We annealed these samples in a variety of oxidizing and reducing atmospheres to obtain overdoped (OD), optimally doped, and underdoped (UD) samples. The $Bi_2Sr_2Cu_1O_{6+\delta}$ (Bi2201) sample studied came from the University of Tokyo and was slightly overdoped. The T_c's of all the samples presented here are listed in Ref. [14].

Figure 1(a) shows the version of Ding *et al.* of the generally accepted holelike FS topology of near-optimal $Bi_2Sr_2CaCu_2O_{8+\delta}$ (Bi2212), from one of the most complete and heavily referenced data sets available [10]. The thick lines represent the FS due to the main CuO_2 band, and thin lines are FS replicas due to the superstructure modulation with a $\vec{Q} = (0.2\pi, 0.2\pi)$. Support for such

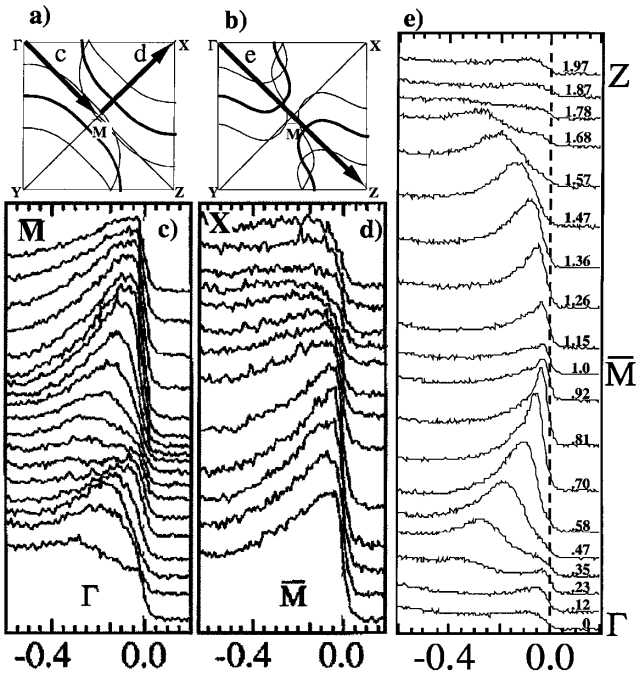

FIG. 1. Normal-state ARPES from Bi2212. (a),(b) One quarter of the Brillouin zone showing (a) the FS extrapolated by Ding *et al.* [10] and (b) the FS determined here. Dark lines are the main FS pieces while the light lines represent superstructure-derived FS replicas. (c),(d) Raw data from Ding taken at $h\nu = 19$ eV along directions indicated in panel (a). (e) A portion of our new data from overdoped sample Bi024 taken at $h\nu = 33$ eV, with each $\vec{k}$-space point listed as a fraction $(x\pi)$ of the Γ-$\bar{M}$ distance.

a topology is displayed in Figs. 1(c) and 1(d). Here we have energy distribution curves (EDCs) from Ding taken at $h\nu = 19$ eV along the high symmetry cuts Γ-$\bar{M}$ and $\bar{M}$-X, where $\Gamma = (0,0)$ and $\bar{M} = (\pi,0)$. From these two panels, the authors claim there is no main band FS crossing along Γ-$\bar{M}$ but that there is one along $\bar{M}$-X, as evidenced by the relatively rapid loss of peak weight in this region.

Figure 1(e) presents a small portion of our new normal-state ARPES data at 33 eV obtained from heavily OD sample Bi-024 along the high symmetry cut Γ-$\bar{M}$-Z [$Z = (2\pi,0)$]. The energy scale for these spectra is the same as in Ding's data of panels 1(c) and 1(d). Clear dispersion is observed with the peak reaching E_F near 0.81π (dark curve). At this same k value, the peak rapidly loses weight, indicating a FS crossing. The peak reappears in the second zone and disperses back towards higher binding energy. Although only a single cut, these data already indicate that there is a fundamental difference between our data at the new photon energy of 33 eV and the previous data of Ding *et al.* Our data indicate main-band FS crossings along Γ-$\bar{M}$-Z, while they are not expected according to the accepted holelike FS topology. In addition, the flat bands (extended vHs) observed near E_F around $\bar{M}$ now have been replaced at 33 eV by a clearly dispersive band which crosses E_F.

To analyze the data in more detail we have made $\vec{k}$-space plots of the integrated spectral intensity $n(\vec{k})$ as well as the weight right at E_F, $A(\vec{k}, E_F)$. We first illustrate how $n(\vec{k})$ and $A(\vec{k}, E_F)$ are expected to behave for a simple bandlike state crossing the FS. Figure 2(a) shows the zero-temperature $n(\vec{k})$ and $A(\vec{k}, E_F)$ for a noninteracting system. In this case there is only weight at $E = E_F$ when $\vec{k} = \vec{k}_F$. In Fig. 2(b) we introduce interactions, which within the Fermi liquid theory framework will reduce both the weight of the delta function peak in $A(\vec{k}, E_F)$ and the step in $n(\vec{k})$ to the value Z (quasiparticle weight). Finite experimental energy and momentum resolution will broaden both curves, as illustrated in Fig. 2(c). Finally, polarization and matrix element effects will slowly alter $n(\vec{k})$, as shown in Fig. 2(d). For panel 2(d) as well as the real data of panels 2(e) through 2(j) it is more accurate to write $M(\vec{k})n(\vec{k})$ and $M(\vec{k})A(\vec{k}, E_F)$ where $M(\vec{k})$ is a $\vec{k}$-dependent matrix element effect, although for brevity we will not make this distinction here. It is clear from the above plots that at a true FS crossing the following criteria should be obeyed: (1) $A(\vec{k}, E_F)$ should be near maximal, dependent somewhat upon the energy resolution and matrix element effects, (2) $n(\vec{k})$ should be near 50% of its maximal value, or equivalently at the maximal gradient point. Also, at E_F we expect (3) the peak dispersion to extrapolate to zero energy, and (4) the midpoint of the leading edge of the spectrum to be at or even beyond (on the unoccupied side of) E_F.

Figures 2(e)–2(j) show the $n(\vec{k})$ and $A(\vec{k}, E_F)$ plots we extracted from our new data on the BSCCO family. To our knowledge, this is the first time that these types of plots have been analyzed together, which turns out

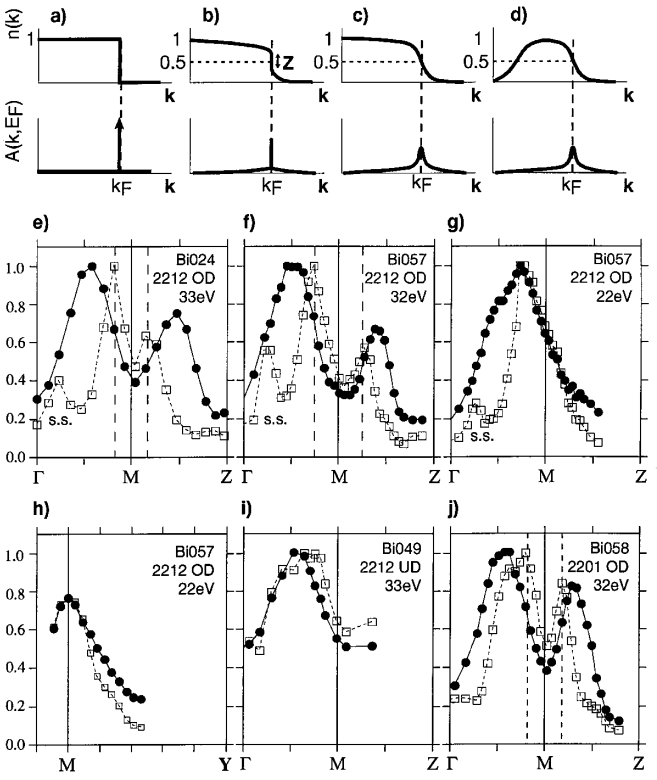

FIG. 2. (a)–(d): Schematics of the expected behavior of $n(\vec{k})$ and $A(\vec{k}, E_F)$ for a band crossing the FS. (a) Noninteracting system at zero temperature. (b) Interacting Fermi liquid with a reduced quasiparticle weight Z. (c) Same as (b) but with finite energy and momentum resolution. (d) Same as (c) but including polarization and matrix element effects. Panels (e)–(j) are $n(\vec{k})$ (circles, solid line) and $A(\vec{k}, E_F)$ (squares, dashed line) at different photon energies from BSCCO samples with varying number of CuO_2 layers and doping levels (indicated on panels). Vertical dashed lines indicate a main-band FS crossing. Superstructure-derived crossings are labeled s.s.

to be a powerful new tool to obtain FS crossings. To determine $n(\vec{k})$ we integrated the ARPES spectral weight from -500 meV to $+100$ meV to span the peak, and for $A(\vec{k}, E_F)$ we integrated over a 50 meV wide window centered at E_F. All plots were normalized so the maximum weight along Γ-$\bar{M}$-Z was set to 1. According to criteria (1) and (2), a FS crossing should occur when $n(\vec{k})$ loses about half of its maximum value (excluding the background) and $A(\vec{k}, E_F)$ simultaneously peaks. These points are indicated in the figure by the vertical dashed lines. Panel 2(e) shows $n(\vec{k})$ and $A(\vec{k}, E_F)$ obtained from the raw data of Fig. 1(e) and panel 2(f) shows data from OD sample Bi057. As expected, criteria (1) and (2) give identical FS crossings as obtained by studying the peak dispersion [criteria (3) and (4)]. Importantly, the drastic drop in $n(\vec{k})$ at $\bar{M}$ to a value comparable to that at Γ or Z indicates that this crossing is due to the main band and not due to a weak superstructure band. Also, the drop in $n(\vec{k})$ at the Z point to a level equivalent to that at the Γ point cannot be explained by photon polarization

or orbital symmetry arguments. Although not central to this paper, this observation includes new physics which warrants further experimental and theoretical attention.

We have taken many cuts over the Brillouin zone at 33 eV on slightly OD sample Bi-031. Within experimental resolution, each of the FS crossing criteria gave identical crossing locations for each cut. The crossing points indicated from these cuts are shown by the white dots in Fig. 3. Thick lines indicate the main FS (stronger ARPES peaks) and thin lines indicating the superstructure-derived FS (ARPES peaks of about 30% the intensity of the main peaks). The superstructure FS's are seen to be replicas of the main FS's, but shifted by $\pm 0.2(\Gamma\text{-}Y)$. We note that the FS topology measured here is closed around the Γ point, in opposition to the "accepted" FS topology of Bi2212 which is closed around the X and Y points.

Despite this discrepancy, there are data in the literature that confirm our new FS topology. Figure 3 shows an overlay of our new FS with an E_F intensity plot from an optimally doped Bi2212 crystal at 33 eV measured by Saini *et al.* [11]. The E_F intensity is analogous to our $A(\vec{k}, E_F)$; i.e., the maximum intensity locations should correspond to FS crossings. The overlay shows a striking similarity between these two independently obtained results. However, instead of interpreting their data as a FS centered around Γ, Saini *et al.* argued that it was still representative of a holelike FS centered around X and Y, and that the loss of weight at $\bar{M}$ was due to a pseudogap in the spectral function. Our experiments and analysis instead attribute the weight loss around $\bar{M}$ to a FS crossing. Indeed, Fig. 1(e) shows that the midpoint of our leading edge is fully up to or even past E_F, and so no pseudogap is observed in these OD samples. A holelike FS plus superstructure effects was also put forth by Mesot *et al.* [15] to explain Saini's data, although we feel that their scenario cannot explain the near-complete weight loss observed at $\bar{M}$ nor the curvature of the FS near $\bar{M}$.

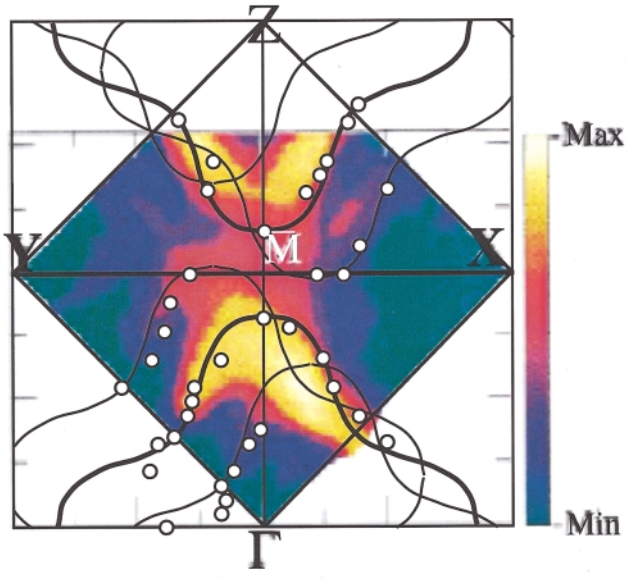

FIG. 3 (color). FS crossing points (white) from 33 eV data on slightly overdoped Bi2212. The thick black lines through the points indicate the main FS and the thin black lines indicate the superstructure-derived FS. Our data are overlayed on a color-scale plot of ARPES intensity at E_F from an optimally doped Bi2212 sample, as measured at 33 eV by Saini *et al.* [11]. The highest intensity regions are yellow and the lowest intensity regions are green.

Figures 2(i) and 2(j) show that the new behavior detailed here is robust as a function of sample type. These plots show $n(\vec{k})$ and $A(\vec{k}, E_F)$ along $\Gamma\text{-}\bar{M}\text{-}Z$ at $h\nu$ near 33 eV for a heavily underdoped sample Bi-049 and for an overdoped single plane (Bi2201) sample Bi-058. In both cases the data indicate a main-band crossing between Γ and $\bar{M}$, indicating that the FS topology should also be closed around Γ (the crossing is more washed out for the underdoped sample, but appears to be qualitatively similar in other respects). This indicates that the new physics shown here is not peculiar to one doping level or sample type. Rather, we argue that it is a product of the new photon energy range used for our measurements, and we are able to obtain different types of behavior on one sample simply by changing the photon energy, as shown in Figs. 2(f) and 2(g).

Changing the photon energy in an ARPES experiment can have a number of effects. For a fixed $k_\parallel$, one obvious effect is that $k_\perp$ will change. We have taken data at many more photon energies to check whether the Fermi surface topology oscillates as a function of $k_\perp$. We find only gradual changes as a function of photon energy without any clear effects with a periodicity in $k_\perp$ of $2\pi/c$ where c is the c-axis lattice constant. Thus we conclude that the differences in the data as a function of photon energy are not naturally linkable to a coherent three-dimensionality of the band structure. This is consistent with the huge in-plane vs out-of-plane transport anisotropy of these materials.

A further important effect of varying the photon energy will be variations in the photoemission matrix elements; i.e., the ARPES intensity is not just a function of the initial state but also of the density and symmetry of the final state bands. At these relatively high photon energies the final state is typically considered to be a continuum with minimal structure. However, detailed calculations taking into account the full band structure do, in fact, show modulations in the matrix elements as a function of $h\nu$ and $k_\parallel$ [16]. It could be argued that the decrease in spectral weight at $\bar{M}$ at 33 eV could be due to a large drop in weight due to matrix element effects. However, if this were the case then we would not expect $A(\vec{k}, E_F)$ to rise as $n(\vec{k})$ dropped. On the other hand, the very asymmetric behavior measured around $\bar{M}$ at 22 eV [Fig. 2(g)] probably indicates that strong matrix element effects are present in these data. Likewise, the simultaneous drop in $n(\vec{k})$ and $A(\vec{k}, E_F)$ as we move from $\bar{M}\text{-}Y$ at 22 eV [Fig. 2(h)] also looks like a matrix element effect, instead of displaying a FS crossing behavior [in which case we expect $A(\vec{k}, E_F)$

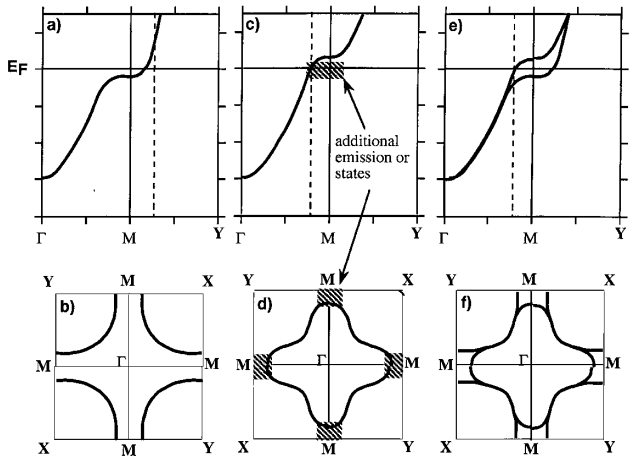

FIG. 4. Schematic diagrams of the E vs $\vec{k}$ relations for near-optimal BSCCO. (a),(b) The old picture of the extended saddle point below E_F. (c),(d) New dispersion relation showing a nonextended saddle point above E_F. We hypothesize additional emission or states near E_F which are visible at 22 eV but not 33 eV, and which sometimes mask the true crossing behavior. (e),(f) Unlikely scenario with two pieces of FS.

to peak near the 50% point of $n(\vec{k})$]. This is important because it is this falloff in $n(\vec{k})$ which had previously been used as evidence for the FS crossing and the hole-pocket topology. Therefore, we argue that the generally accepted picture illustrated in Figs. 4(a) and 4(b) is unlikely to represent the actual physics. Rather, we propose the scenario in Figs. 4(c) and 4(d). The main-band dispersion is as we have measured at 33 eV, and is centered around Γ with a smaller saddle point at $\bar{M}$ above E_F. Additionally, there is extra emission near E_F at $\bar{M}$ which is observed at 22 eV but not 33 eV. At 22 eV this extra emission acts to mask the true crossing behavior of the bands observed at 33 eV, giving the impression of a holelike FS.

It could be argued that two FS's exist in these compounds due to bilayer-split CuO_2 bands, as depicted in Figs. 4(e) and 4(f). However, if this was this case we do not expect Bi2201 samples to display the behavior of Fig. 2(j) at 33 eV and the flat bands at 22 eV [4]. Further, the lack of a nice crossing behavior of the "holelike" portion makes us hesitant to call this portion a real FS crossing [Fig. 2(h)]. Rather, there seems to be extra emission or an extra electronic component of some as yet undetermined origin. Possible origins include (1) leakage from the states above E_F if they have a linewidth large compared to their energy above E_F and a greatly enhanced intensity due to matrix element effects, (2) a contribution from the Bi-O states [17,18], (3) photoelectron diffraction effects [19], or (4) new states due to quantum confinement due to charge stripe formation [20] or a new type of correlated electron state due, for instance, to magnetism. Whatever the origin, this extra emission has repeatedly shown superconducting gaps and for underdoped samples pseudogaps, as do the states observed at 33 eV [21].

The new FS topology as well as the position of the vHs should have a number of implications for our understanding of the diverse and unusual properties of the cuprates. As an example we mention the Hall effect. In the FS topology proposed here, the portion of the FS near $\bar{M}$ will give an electronlike contribution, while the portions near the zone diagonal will give holelike contributions. These will partially cancel each other, likely making the Hall coefficient more sensitive to variations in the scattering rates (e.g., with temperature) from the different FS portions. This may help explain the relatively low values of the Hall coefficient often observed, as well as why they are so sensitive to temperature.

We acknowledge helpful conversations with Arun Bansil, Matti Lindroos, and Andy Millis, as well as support from the Office of Naval Research's Young Investigator Program. The SRC is supported by NSF Contract No. DMR-95-31009, and SSRL is operated by the Department of Energy, Office of Basic Energy Sciences. We thank Aharon Kapitulnik for the use of one Bi2212 sample.

Note added.—The results of this paper have recently been confirmed by D. L. Feng *et al.*, http://xxx.lanl.gov/abs/cond-mat/9908056.

[1] Z.-X. Shen and D. S. Dessau, Phys. Rep. **253**, 1 (1995).
[2] D. S. Dessau *et al.*, Phys. Rev. Lett. **71**, 2781 (1993).
[3] K. Gofron *et al.*, Phys. Rev. Lett. **73**, 3302 (1994).
[4] D. M. King *et al.*, Phys. Rev. Lett. **73**, 3298 (1994).
[5] Z.-X. Shen *et al.*, Phys. Rev. Lett. **70**, 1553 (1993).
[6] H. Ding *et al.*, Phys. Rev. B **54**, R9678 (1996).
[7] A. G. Loeser *et al.*, Science **273**, 325 (1996).
[8] D. S. Marshall *et al.*, Phys. Rev. Lett. **76**, 4841 (1996).
[9] H. Ding *et al.*, Nature (London) **382**, 51 (1996).
[10] H. Ding *et al.*, Phys. Rev. Lett. **76**, 1533 (1996).
[11] N. L. Saini *et al.*, Phys. Rev. Lett. **79**, 3467 (1997).
[12] P. Aebi *et al.*, Phys. Rev. Lett. **72**, 2757 (1994).
[13] At both labs we used 50 mm hemispherical energy analyzers mounted on two-axis goniometers. Total energy resolution was about 50 meV FWHM, angular resolution was $\pm 1°$ and the temperature was at 100 K. Base pressure was about 10^{-10} torr for the SRC system and better than 3×10^{-11} torr for the SSRL system.
[14] $T_c, \Delta T$ for BSCCO are as follows: Bi-024 T_c around 50–60 K, determined spectroscopically; Bi-057 $T_c = 83$ K, $\Delta T = 2.5$ K; Bi-031 $T_c = 87$ K, $\Delta T = 3$ K; Bi-049 $T_c = 10$–20 K; Bi-058 had $T_c = 8$ K, $\Delta T = 2$ K.
[15] J. Mesot *et al.*, Phys. Rev. Lett. **82**, 2618 (1999).
[16] A. Bansil and M. Lindroos, J. Phys. Chem. Solids **59**, 1879 (1998).
[17] B. O. Wells *et al.*, Phys. Rev. Lett. **65**, 3056 (1990).
[18] S. Massida *et al.*, Physica (Amsterdam) **152C**, 251 (1988).
[19] C. Fadley, in *Synchrotron Radiation Research*, edited by R. Bachrach (Plenum, New York, 1992).
[20] Z-X Shen, S. Maekawa, and T. Tohyama (private communication).
[21] A. Gromko *et al.* (to be published).